http://dx.doi.org/10.5012/bkcs.2011.32.10.3730

Thickness Dependence of Size and Arrangement in Anodic TiO_2 Nanotubes

Sunmi Kim, Byung Gun Lee, and Jinsub Choi*

*Department of Chemical Engineering, Inha University, Incheon 402-751, Korea. *E-mail: jinsub@inha.ac.kr*
Received July 17, 2011, Accepted August 10, 2011

The degree of self-assembly and the size variation of nanotubular structures in anodic titanium oxide prepared by the anodization of titanium in ethylene glycol containing 0.25 wt % NH_4F at 40 V were investigated as a function of anodization time. We found that the degree of self-assembly and the size of the nanotubes were strongly dependent on thickness deviation and thus indirectly on anodization time, as the thickness deviation was caused by the dissolution of the topmost tubular structures at local areas during long anodization. A large deviation in thickness led to a large deviation in the size and number of nanotubes per unit area. The dissolution primarily occurred at the bottoms of the nanotubes (D_{bottom}) in the initial stage of anodization (up to 6 h), which led to the growth of nanotubes. Dissolution at the tops (D_{top}) was accompanied by D_{bottom} after the formed structures contacted the electrolyte after 12 h, generating the thickness deviation. After extremely long anodization (here, 70 h), D_{top} was the dominant mode due to increase in pH, meaning that there was insufficient driving force to overcome the size distribution of nanotubes at the bottom. Thus, the nanotube array became disorder in this regime.

Key Words : Anodization, Titanium oxide, Dissolution, Thickness variation

Introduction

Following great success in the fabrication of anodic aluminum oxide (AAO) and its application in various fields,[1-4] many valve metals such as Ti,[5-10] W,[11-14] Ta,[15-17] Nb[18,19] and their alloys have been intensively investigated in attempts to fabricate materials analogous to AAO. Nanotubular anodic titanium oxide (ATO) with a high aspect ratio have been considered to be a worthy successor to AAO since it exhibits similar highly regular nanostructures in a self-assembled manner.[5-10]

Because many theories on the principles of the fabrication of highly ordered AAO have been well established for number of years,[20-25] their knowledge should be very useful in obtaining a deeper understanding of the anodization process in the fabrication of ATO. The influence of anodization time on the length of the nanotubes and the relationship between the interpore distance and the applied potential within certain ranges have been studied to this end.[26-28] In addition, it was reported that AAO and ATO prepared below breakdown potential are usually an amorphous structure irrespective of anodizing time.[26,28] The amorphous structure of AAO and ATO can be converted to crystalline structures by annealing under appropriate conditions.[28-29]

A diameter-potential dependency in ATO was recently reported by several groups.[30-33] In addition, it has been reported that the length of ATO reaches a maximum in terms of anodizing time and then reaches a steady state due to etching.[34-37]

Contributing to the efforts to generalize the mechanism of the anodic growth of nanostructures, we performed comparative studies on electropolishing effects in the growth of AAO and ATO and their stepwise reduction behaviors during thinning.[38] In this study, the degree of self-assembly and the size and number of nanotubes in ATO were investigated in terms of thickness changes, considering that the diameter of AAO nanotubes is usually determined by the applied potential, and the degree of self-assembly linearly improves up to the diffusion limit length.[39]

Experimental

A Ti foil with a thickness of 0.127 mm (99.7%, Aldrich, USA) was used as the starting substrate for the fabrication of highly ordered ATO. First, the foil was degreased by sonicating in acetone and then in isopropanol, followed by rinsing with deionized (DI) water. Subsequently, the foil was dried in a nitrogen stream with no additional surface polishing. The anodization was carried out using a power supply (SourceMeter 2400, Keithley) interfaced with a computer at a constant potential of 40 V for varying durations at room temperature. An ethylene glycol (99.8%, Aldrich, USA) solution containing 0.25 wt % NH_4F was used as the electrolyte. The anodization setup consisted of a conventional two-electrode configuration with a platinum mesh as the counter electrode and the cleaned titanium foil as the working electrode. During the anodization, 10 mL of electrolyte was taken for pH measurement (Orion 2-Star pH Benchtop Meter, Thermo Scientific). After pH measurement, the electrolyte was added into the original electrolyte. After forming the nanotubular structures, specimens were immediately rinsed with DI water and then dried in a nitrogen stream. Field emission scanning electron microscopy (FE-SEM, 4300S, Hitachi, Japan) was employed for the structural and morphological characterization. Film thickness was measured

directly from the cross-sectional images.

Results and Discussion

According to Raja *et al*.,[40] anodic growth of nanotubes in EG can be explained by the balance between oxide formation and oxide dissolution.

Ti is oxidized into TiO_2 in EG through the several steps of reactions at anode:[40]

$$2(CH_2OH) + TiO_2 \text{ (air formed film)} \rightarrow Ti + 2(COOH\text{-}CH_2OH) + 4H^+ + 4e^- \quad (1)$$

$$COOH\text{-}R \rightarrow (R\text{-}COO)^- + H^+ + e^- \quad (2)$$

$$Ti + 4(R\text{-}COO)^- \rightarrow (RCOO)_4Ti + 4e^- \quad (3)$$

$$(RCOO)_4Ti \rightarrow TiO_2 + CO_2 + nH^+ ne^- \quad (4)$$

In addition, dissolution of the formed oxide takes a place at the bottom of TiO_2 and/or at the tops of the nanotubes by the following reaction:

$$TiO_2 + 4H^+ + 6F^- \rightarrow TiF_6^{2-} + 2H_2O \quad (5)$$

At cathode, hydrogen ions dissociated from anodically produced H_2O are reduced into hydrogen gas, leaving OH- ions in the electrolyte. The probably increase pH in the solution.

$$H^+ + H^+ \rightarrow H_2 \uparrow \quad (6)$$

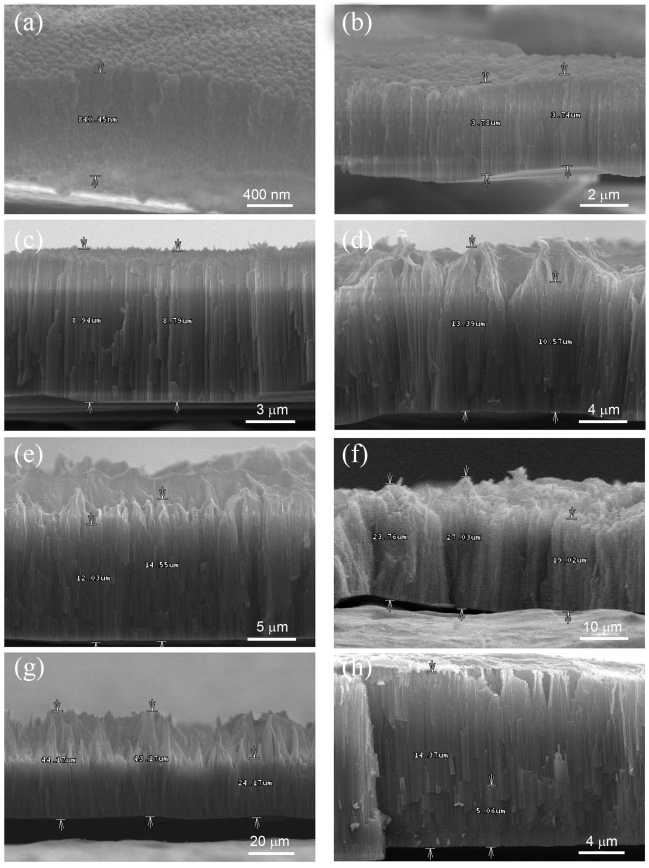

Figure 1. Cross-sectional SEM images of TiO_2 nanotubes prepared at 40 V in ethylene glycol containing 0.25 wt % NH_4F for different anodizing times: (a) 1 h, (b) 3 h, (c) 6 h, (d) 12 h, (e) 48 h, (g) 60 h, and (h) 72 h.

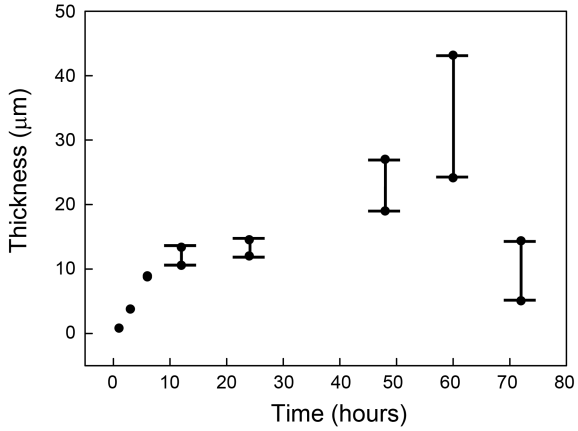

Figure 2. Thickness and thickness deviation of TiO_2 nanotubes at different anodizing times.

Figure 1 shows cross-sectional images of ATO prepared at 40 V with different anodization times, suggesting that the thickness did not linearly increase with anodizing time. Due to surface dissolution during anodization (reaction 5), the thickness deviation increased as a function of anodizing duration. Figure 2 shows the thickness deviations versus anodizing time, demonstrating that the thickness deviations in ATO prepared at 6 h were from a few tens of nanometers to a few hundreds of nanometers. The bars depicted after 12 h means the deviation of thickness at area-by-area in one sample, indicating that a distinct thickness deviation of more than 3 μm was observed at 12 h, and it further increased to 20 μm at 60 h. Interestingly, both the thickness and thickness deviation significantly decreased at 72 h. This significant thickness reduction after long anodization has not been reported in the literature. For example, Grimes's group reported that nanotubes can be grown up to 1,005 μm thick at 60 V for 9 days.[28] It is probably due to different anodization conditions. Since the anodization condition in this work makes narrow nanotubes, a diffusion problem leads to relatively short length of nanotubes.

The nonlinear thickness deviation can be explained by two different dissolution modes[10,41]: one for the formation of titanium oxide nanotubes, which primarily occurs at the bottoms of the nanotubes (D_{bottom}), and a second ascribed to the dissolution of the formed oxide, which mainly takes place at the tops of the nanotubes (D_{top}), which are in contact with the electrolyte for the longest time. During the initial growth of nanotubular structures, it is clear that D_{bottom} is dominant; otherwise, the nanotubes could not be produced. If anodization is conducted for more than 12 h, both D_{bottom} and D_{top} become important modes due to the continuous dissolution of nanotube walls. Thus, the thickness deviation linearly increased as a function of the anodizing time at this stage. Finally, D_{top} develops into the dominant mode after extremely long durations (here 72 h). Due to long anodization, amount of H^+ and OH^- are produced by the dissolu-

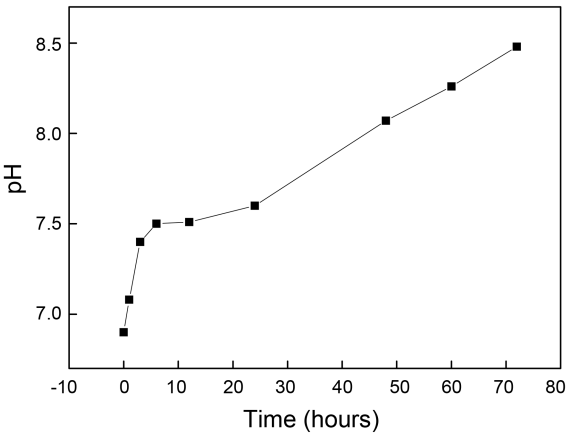

Figure 3. Variations of pH values in the electrolyte as a function of anodizing time.

tion of TiO_2 through reaction (5). As mentioned earlier, the hydrogen ions are consumed into hydrogen gas in the cathode, leaving the OH^- ions. Since the anodic nanotubes can be grow up at localized low pH condition,[6] extreme increase in pH value around the mouth of nanotubes probably makes stop (or weak) the growth of nanotubes at the bottom. Figure 3 shows pH variation during anodization, indicating that the concentration of OH^- ions increases as a function of anodization time as we explained.

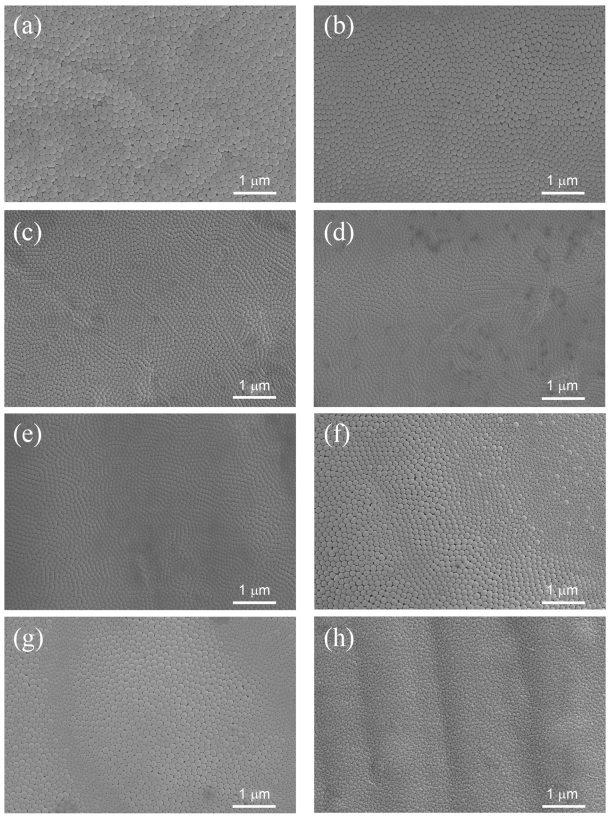

Figure 4. Bottom views of SEM images of TiO_2 nanotubes prepared at 40 V in ethylene glycol containing 0.25 wt % NH_4F for different anodizing times: (a) 1 h, (b) 3 h, (c) 6 h, (d) 12 h, (e) 48 h, (g) 60 h, and (h) 72 h.

From the results, the critical point that D_{bottom} becomes very weak is probably pH 8.2 in bulk EG electrolyte.

Evidence that D_{top} was the dominant mode after the extreme long anodization was provided by the bottom views of the ATO. Figure 4 shows FE-SEM images of the bottoms of the ATO at different anodization times, clearly demonstrating that the degree of ATO self-assembly did not improve with anodizing time. As the anodization time was increased up to 6 h (Figures 4(a), (b) and (c)), the arrangement of the nanotubes slightly improved. Subsequently, it began to degenerate (Figures 4(d)-(g)) because nanotubes of different sizes were generated. At 72 h, tiny, disordered nanotubes were observed (Figures 4(h)), indicating that D_{bottom} became very weak (D_{top} mode). Note that this variation in ATO nanotube size with anodizing time was very interesting finding, as the pore size of AAO is usually constant during anodization.

Overall, as anodization time was increased up to 12 h, the size of the nanotubes decreased, as shown in Figure 5(a). This effect was attributed to the increase in diffusion length of ions. After 24 h, nanotubes of distinctly different sizes were observed ((Figures 4(e)-(g) and Figure 5(a)). The size deviations increased until 60 h, with a difference as great as 1.5×10^4 nm^2. The sizes of the nanotubes and their deviation then significantly decreased at 72 h (Figure 4(h)). At this stage, tiny, disordered nanotubes were produced. In contrast, the number of nanotubes increased until 12 h (Figure 4(b)). The number of nanotubes then differed from one area to the

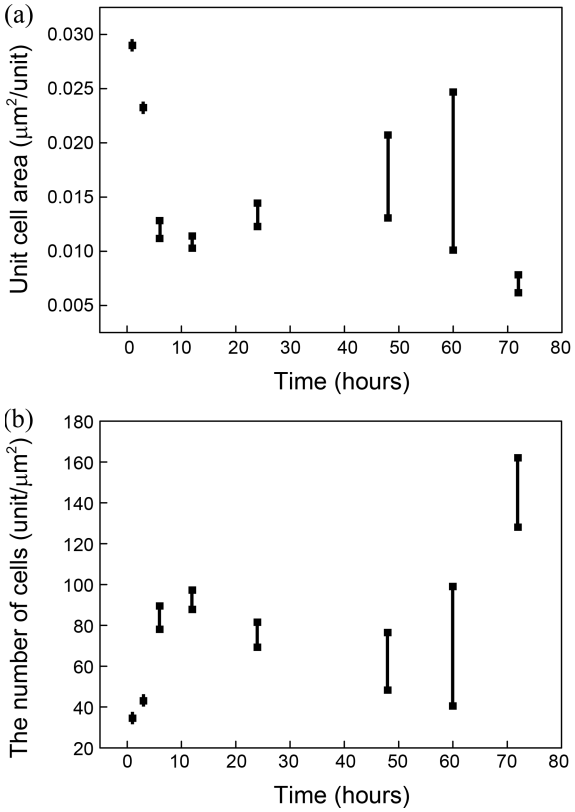

Figure 5. Variations of (a) nanotubes size and (b) number at different anodizing times.

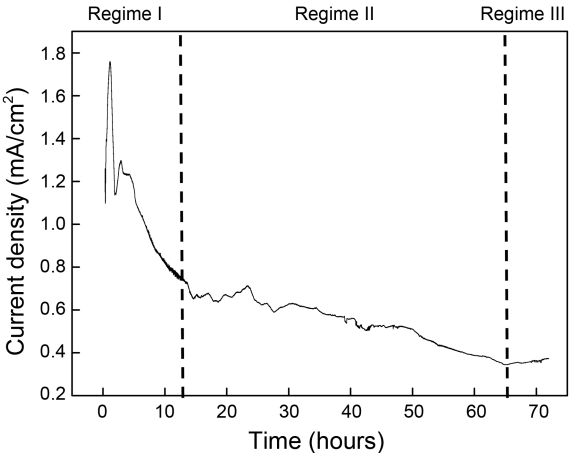

Figure 6. Current-time transient during the fabrication of nanotubular TiO_2. There are three regimes: a decrease in current (Regime I), a fluctuation in current (Regime II), and an increase in current (Regime III).

next within the same sample, meaning that there was a significant deviation in the number of nanotubes per unit area. The changes in the size and the number of nanotubes shown in Figure 5 were very well correlated with the thickness deviation in Figure 2, meaning that the number and size of nanotubes and the degree of self-assembly were strongly dependent not on anodizing time but rather on thickness and thickness deviation.

This observation reports a very different behavior from that of AAO: in AAO production, pores are randomly initiated on the surface based on an electric-field enhanced dissolution mechanism.[42] The randomly over-nucleated pores are adjusted to a well-distributed number of pores as some pores stop growing, showing a self-assembly character ascribed to mechanical stress caused by the volume expansion when aluminum is converted into aluminum oxide. Thus, the degree of self-assembly improves as the anodization proceeds. However, if the anodization is conducted for too long, the self-assembled arrays degenerate due to diffusion problems in the extremely long nanopores. Thus, there is a maximum thickness displayed by the most-ordered AAO.[41,43]

Figure 6 shows the current transients during the formation of ATO, suggesting that there were three dissolution regimes, as we observed: the current reduction regime (Regime I), the fluctuation regime (Regime II), and the slight current increase (Regime III). As a decrease in current density indicates the growth of nanotubes (Regime I), the nanotubes grew linearly up to 10 h. After 12 h, there was a fluctuation of current density (Regime II), indicating the occurrence of a significant thickness deviation. After 65 h, a slight increase in current density was observed. As mentioned above, the growth rate of nanotubes due to D_{bottom} was very weak in this regime.

Conclusions

In this report, we described how the self-assembly, as well as the size and number of nanotubes, was strongly influenced not directly by anodizing time but rather by thickness and thickness deviation. We found that there were three dissolution regimes influencing the size and number of nanotubes and their self-assembly: In the first regime, where there was no significant surface dissolution by D_{top}, the self-assembly of ATO and the thickness of nanotubes improved and increased, respectively, as the anodization time was increased. The increase in the thickness led to a reduction in the size of the nanotubes and an increase in their number per unit area. In this regime, constant current reduction was observed in the current-time transient graph. In the second regime, showing a fluctuation in the current-time transient graph, ATO was rapidly dissolved due to D_{top}, causing a significant thickness deviation. This deviation led to remarkable differences in the size and number of nanotubes from one area to the next, degenerating the self-assembly. Finally, the nanotubes became completely disordered in the regime where D_{top} was the dominant mode rather than D_{bottom}. Dtop dominant mode was attributed to increase in pH value due to the dissolution of TiO_2 and hydrogen reduction reaction at cathode. At more than pH of 8.2, D_{bottom} became very weak to grow pores. In this regime, the current increased slightly.

Acknowledgments. This research was supported by the Basic Science Research Program through the National Research Foundation of Korea (NRF) and funded by the Ministry of Education, Science and Technology (2010-0011197) and was supported by an Inha University Research Grant.

References

1. Nielsch, K.; Müller, F.; Li, A. P.; Gösele, U. *Adv. Mater.* **2000**, *12*, 582.
2. Steinhart, M.; Wendorff, J. H.; Greiner, A.; Wehrspohn, R. B.; Nielsch, K.; Schilling, J.; Choi, J.; Gösele, U. *Science* **2002**, *296*, 1997.
3. Lakshmi, B. B.; Patrissi, C. J.; Martin, C. R. *Chem. Mater.* **1997**, *9*, 2544.
4. Che, G.; Lakshmi, B. B.; Fisher, E. R.; Martin, C. R. *Nature* **1998**, *393*, 346.
5. Grimes, C. A. *J. Mater. Chem.* **2007**, *17*, 1451.
6. Macák, J. M.; Schmuki, P. *Electrochim. Acta* **2006**, *52*, 1258.
7. Macák, J. M.; Tsuchiya, H.; Ghicov, A.; Schmuki, P. *Electrochem. Commun.* **2005**, *7*, 1133.
8. Macák, J. M.; Tsuchiya, H.; Schmuki, P. *Angew. Chem. Int. Ed.* **2005**, *44*, 2100.
9. Macák, J. M.; Tsuchiya, H.; Taveira, L.; Aldabergerova, S.; Schmuki, P. *Angew. Chem. Int. Ed*. **2005**, *44*, 7463.
10. Mor, G. K.; Varghese, O. K.; Paulose, M.; Shankar, K.; Grimes, C. A. *Sol Energy Mater. Sol. Cells* **2006**, *90*, 2011.
11. Di Quarto, F.; Di Paola, A.; Sunseri, C. *Electrochim. Acta* **1981**, *26*, 1177.
12. Guo, Y.; Quan, X.; Lu, N.; Zhao, H.; Chen, S. *Environ. Sci. Technol.* **2007**, *41*, 4422.
13. Hahn, R.; Macák, J. M.; Schmuki, P. *Electrochem. Commun.* **2007**, *9*, 947.
14. Mukherjee, N.; Paulose, M.; Varghese, O. K.; Mor, G. K.; Grimes, C. A. *J. Mater. Res.* **2003**, *18*, 2296.
15. Allam, N. K.; Feng, X. J.; Grimes, C. A. *Chem. Mater.* **2008**, *20*, 6477.

16. Ueno, K.; Abe, S.; Onoki, R.; Saiki, K. *J. Appl. Phys*. **2005**, *98*, 114503.
17. Wei, W.; Macák, J. M.; Schmuki, P. *Electrochem. Commun.* **2008**, *10*, 428.
18. Choi, J.; Lim, J. H.; Lee, J.; Kim, K. J. *Nanotechnology* **2007**, *18*.
19. Sieber, I.; Hildebrand, H.; Friedrich, A.; Schmuki, P. *Electrochem. Commun.* **2005**, *7*, 97.
20. Diggle, J. W.; Downie, T. C.; Goulding, C. W. *Chem. Rev.* **1969**, *69*, 365.
21. Jessensky, O.; Müller, F.; Gösele, U. *Appl. Phys. Lett.* **2009**, *72*, 1173.
22. Masuda; Fukuda, K. *Science* **1995**, *268*, 1466.
23. O'sullivan, J. P.; Wood, G. C. *Proc. R. Soc. A* **1970**, *317*, 511.
24. Jessensky, O.; Müller, F.; Gösele, U. *J. Electrochem. Soc.* **1998**, *145*, 3735.
25. Thompson, G. E.; Xu, Y.; Skeldon, P.; Shimizu, K.; Han, S. H.; Wood, G. C. *Philos. Mag. B* **1986**, *55*, 651.
26. Choi, J.; Wehrspohn, R. B.; Lee, J.; Gösele, U. *Electrochim. Acta* **2004**, *49*, 2645.
27. Nguyen, Q. A. S.; Bhargava, Y. V.; Devine, T. M. *J. Electrochem. Soc.* **2009**, *156*, 3.
28. Grimes, C. A.; Mor, G. K. *Springer* 2009; pp 1-66.
29. Diggle, J. W.; Downie, T. C.; Coulding, C. W. *Chem. Rev.* **1969**, *69*, 365.
30. Yasuda, K.; Macák, J. M.; Berger, S.; Ghicov, A.; Schmuki, P. *J. Electrochem. Soc.* **2007**, *154*, 9.
31. Sun, L.; Zhang, S. Sun, X. W.; He, X. *J. Electroanal. Chem.* **2009**, *637*, 6.
32. Meng, X.; Lee, T. Y.; Chen, H.; Shin, D. W.; Kwon, K. W.; Kwon, S. J.; Yoo, J. B. *J. Electrochem. Soc*. **2010**, *10*, 4259.
33. Sulka, G. D.; Kapusta-Kołodziej, J.; Brzózka, A.; Jaskuła, M. *Electrochim. Acta* **2010**, *55*, 4359.
34. Berger, S.; Hahn, R.; Roy, P.; Schmuki, P. *Phys. Status Solidi B (b)* **2010**, *247*, 2424.
35. Shankar, K.; Mor, G. K.; Prakasam, H. E.; Yoriya, S.; Paulose, M.; Varghese, O. K.; Grimes, C. A. *Nanotechnology* **2007**, *18*, 6.
36. Tang, X.; Li, D. *J. Phys. Chem. C* **2009**, *113*, 7107.
37. Berger, S.; Kunze, J.; Schmuki, P.; LeClere, D.; Valota, A. T.; Skeldon, P.; Thompson, G. E. *Electrochim. Acta* **2009**, *54*, 5942.
38. Lee, B. G.; Hong, S. Y.; Yoo, J. E.; Choi, J. *Appl. Surf. Sci*. **2010**, *257*, 7190.
39. Nielsch, K.; Choi, J.; Schwirn, K.; Wehrspohn, R. B.; Gösele, U. *Nano Lett*. **2002**, *2*, 7.
40. Raja, K. S.; Gandhi, T.; Misra, M. *Electrochem. Commun.* **2007**, *9*, 1069.
41. Macák, J. M.; Tsuchiya, H.; Schmuki, P. *Angew. Chem. Int. Ed*. **2005**, *44*, 2100.
42. Su, Z.; Zhou, W. *Adv. Mater*. **2008**, *20*, 3663.
43. Parkhutik, P.; Shershulsky, V. I. *J. Phys. D* **1992**, *25*, 1258.